Biomarker Insights

ORIGINAL RESEARCH

^{1}H HRMAS NMR Derived Bio-markers Related to Tumor Grade, Tumor Cell Fraction, and Cell Proliferation in Prostate Tissue Samples

Katarina Stenman[1], Pär Stattin[3], Hans Stenlund[4], Katrine Riklund[1], Gerhard Gröbner[5] and Anders Bergh[2]

[1]Departments of Radiation Sciences, Diagnostic Radiology, [2]Medical Biosciences, Pathology, [3]Surgical and Perioperative Sciences, Urology and Andrology, [4]Public Health and Clinical Medicine, Epidemiology, Umeå University and University Hospital of Northern Sweden, Umeå, Sweden. [5]Department of Chemistry, Umeå University, Umeå, Sweden. Corresponding author email: katarina.stenman@sidb.diagrad.umu.se

Abstract: A high-resolution magic angle spinning NMR spectroscopic approach is presented for evaluating the occurrence, amount and aggressiveness of cancer in human prostate tissue samples. Using this technique, key metabolites in malignant and non-malignant samples (n = 149) were identified, and patterns of their relative abundance were analyzed by multivariate statistical methods. Ratios of various metabolites – including (glycerophophorylcholine + phosphorylcholine)/creatine, myo-inositol/scyllo-inositol, scyllo-inositol/creatine, choline/creatine, and citrate/creatine – correlated with: i) for non-malignant tissue samples, the distance to the nearest tumor and its Gleason score and; ii) the fraction of tumor cells present in the sample; and iii) tumor cell proliferation (Ki67 labelling index). This NMR-based approach allows the extraction of information that could be useful for developing novel diagnostic methods for prostate cancer.

Keywords: prostate cancer, HRMAS, MRSI, inositol, Gleason score, Ki67

Biomarker Insights 2011:6 39–47

doi: 10.4137/BMI.S6794

This article is available from http://www.la-press.com.

Introduction

Prostate cancer (PCa) is among the most common cancers diagnosed worldwide.[1] The course of the disease is highly variable and very difficult to predict at diagnosis using currently available techniques.[2] New diagnostic procedures are urgently needed that can accurately detect non-palpable tumors,[3] increase biopsy sensitivity, differentiate between clinically significant and non-significant variants, and direct biopsies towards the most malignant foci.[4,5] Innovative diagnostic approaches that can meet these requirements are being developed using ex-vivo High Resolution Magic Angle Spinning (HRMAS) NMR,[6–8] and in-vivo magnetic resonance spectroscopic imaging (MRSI).[9,10] Since it is non-destructive, samples analyzed by HR-MAS NMR can be subsequently examined histopathologically.[11–13] Hence, HRMAS NMR-derived scores for metabolic biomarkers can be correlated with standard pathological diagnostics such as the Gleason score,[14] and immunohistochemically-scored prognostic markers such as the Ki67 proliferation index.[7,13] The results can then be used to guide and assist interpretation of results of in-vivo magnetic resonance spectroscopic imaging (MRSI)[15] for clinical studies.

Here, we provide evidence that HRMAS NMR measurements of (glycerophophorylcholine + phosphorylcholine)/creatine (GPCho + PCho)/Cre), myo-inositol/scyllo-inositol (m-Ino/s-Ino), scyllo-inositol/creatine (s-Ino/Cre) and choline/creatine (Cho/Cre) ratios correlate to the fraction of tumor cells in prostate specimens. The method can also provide indications of tumor aggressiveness and the distance of samples from the nearest tumor. Hence, it may have substantial diagnostic potential.

Materials and methods

Source of material and preparation

Samples (149; 108 non-malignant and 41 malignant) obtained from 40 patients ($n = 2–20$ samples from each patient) who had undergone radical prostatectomy for PCa were included in this study. The ages of the patients were 60 ± 5.5 yrs (Mean ± SD; range 41–71 yrs). The pathological tumor stage (pT) ranged from 1 to 3 and their serum prostate-specific antigen (PSA) levels were 12.4 ± 13.5 (Mean ± SD) ng/mL (range 3.0–50). The tumors were all Gleason score 6–7; GS 6 (3 + 3) $n = 27$, and GS (3 + 4) $n = 14$. The patients had not received any anti-cancer treatment prior to surgery. Directly after surgery each specimen was chilled on ice. At pathology prostate surfaces were inked and the prostates were cut into approximately 1-cm thick horizontal sections. From these sections 2–20 samples were punched from the peripheral zone of each prostate. The punches (0.5 cm in diameter and about 1 cm long) were snap-frozen in liquid nitrogen within 30 minutes of surgical removal of the prostate and thereafter stored at −70 °C. The prostate slices were fixed in formalin, embedded in paraffin and cut into 5-µm thick sections. The sections were then stained with hematoxylin and eosin and all tumor foci were identified by microscopy and marked on the whole-mount sections. The origin of each frozen punch could thus be identified on the whole-mount sections as round holes and preliminarily classified as malignant or non-malignant tissue, depending on the type of tissue seen in the immediate surroundings. From each frozen punch a small sample was randomly cut and analyzed by HRMAS as described below. After HRMAS each analyzed sample was fixed in formalin, embedded in paraffin, cut into 5 µm thick sections, and immunostained for high molecular weight cytokeratin (cytokeratin-hmw, DAKO, Stockholm, Sweden) or the cell proliferation marker Ki67 (DAKO) as previously described,[16] using standard histopathological procedures. In these sections the percentage of tumor tissue (glands lacking cytokeratin-hmw positive basal epithelial cells) and non-malignant tissue (glands with an intact basal epithelial cell layer) and the tumor Gleason score were determined. The fraction of malignant vs. non-malignant tissue in each sample was determined by using a light microscope with a square-lattice mounted in the eye-piece to count the number of grid-intersections falling on each tissue compartment, as previously described.[17] The distance between each sample of non-malignant prostate tissue and the closest tumor was also measured on the whole mount sections of the prostates. The study design was approved by the review board for human studies in Umeå, Sweden.

^{1}H HRMAS NMR experiments

NMR spectroscopy was performed using an AMX2 NMR spectrometer operating at a ^{1}H frequency of

500.13 MHz, equipped with a HRMAS dual band (^{1}H and ^{13}C) probe and 4 mm zirconia rotors with spherical inserts and Kel-F caps (all from Bruker Biospin GMBH, Karlsruhe, Germany). All prostate specimens were cut into 15 ± 5 mg portions using a surgical steel blade to fit the rotors, 10 µl of D_2O was added to each specimen for ^{2}H field locking, then the samples were packed in rotors and either immediately analyzed or temporarily stored at −20 °C. All samples were treated as identically as possible to minimize handling errors, and spun at constant room temperature (20 °C), at 5 kHz and the magic angle (54.7°). A rotor-synchronized Carr-Purcell-Meibom-Gill (CPMG) pulse sequence, $90°-(\tau-180°-\tau)_n$-acquisition,[18] with a T_2 filter of 20 ms duration was used to suppress broad signals from macromolecules. Each spectrum was recorded with 256 transients, using 16 K complex time domain data points and a spectral width of 10309 Hz at a repetition time of 5.0 seconds. Water signals were suppressed with a presaturation pulse during the relaxation delay prior to the CPMG pulse sequence. All 1D spectra were generated at a maximum time of 30 minutes.

Spectral processing

All NMR spectra were processed using MestReNova 6.0.4 (Mestrelab Research, A Coruña, Spain). The free induction decays (FID's) of the CPMG-edited ^{1}H HRMAS spectra were subjected to a 1.5 Hz exponential multiplication prior to Fourier transformation. The spectra were referenced to the residual water peak by setting the chemical shift of the lactate doublet equal to exactly 1.33 ppm.

Statistics

Lactate and alanine signals from the prostate samples were found to be somewhat unstable,[19] possibly due to oxidation in contact with air, and their lipid contents were found to be highly variable, thus these substances were excluded from further analysis. However, HRMAS NMR integrals indicating levels of (GPCho + PCho), choline, citrate, creatine, taurine, myo-inositol and scyllo-inositol were more constant. Summary statistics for these variables (means and SD) were calculated using SPSS v. 16.0 (SPSS, Chicago, IL, USA). Relationships between these potentially predictive variables and the cancer status of the samples were then examined using STATA (v. 10, StataCorp LP, College Station, TX, USA), in which the data were initially standard error-adjusted, to take dependencies between samples originating from the same patient (clustering) into consideration. The ability of Cit/Cre, m-Ino/s-Ino, and Cho/Cre ratios to discriminate between prostate tissue specimens (malignant and non-malignant) with Gleason scores of 6 (3 + 3) and 7 (3 + 4) was assessed by binary logistic regression. In addition, multivariate linear regression was then applied to assess the relationships between: the tumor fraction in the tissue samples (% cancer), where the tumor fractions were grouped into bins of; 0%, 20%, 40%, 60%, 80%, and 100%, distance to tumor, and Ki67 (dependent variables), and the following metabolic ratios: (GPCho + PCho)/Cre, Cho/Cre, m-Ino/s-Ino, and s-Ino/Cre. When employing tumor fraction bins as dependent the predictors corresponding metabolic mean ratios were used. In all of these analyses, *P*-values ≤ 0.05 were considered to be statistically significant.

Results

^{1}H HRMAS NMR spectra of prostate tissues

As shown in Figure 1, well-resolved 1D ^{1}H HRMAS NMR spectra were obtained from the prostatectomy material (within 30 minutes for each spectrum). None of the samples appeared to be adversely affected by the fast spinning rate and they could be successfully examined by histopathology post HRMAS NMR. Various metabolites were detected in the NMR spectra of non-malignant (Fig. 1A) and malignant prostate tissues (10% malignant, Fig. 1B; 100% malignant, Fig. 1C; corresponding morphological pictures are presented on the left side of each NMR spectrum), as indicated, including: lactate (1.33 ppm), alanine (1.48 and 3.78 ppm), glutamate (2.05, 2.15, and 2.35 ppm), glutamine (2.14 and 2.47 ppm), citrate (2.55 and 2.65 ppm), diallylic protons (omega-6,[20] 2.80 ppm), creatine (3.02 and 3.94 ppm), polyamines (3.05–3.15 ppm), choline (3.20 ppm), glycerophosphorylcholine + phosphorylcholine (GPCho + PCho, 3.22 ppm), taurine (3.25 and 3.46 ppm), myo-inositol (3.29 and 3.52–3.62 ppm) and scyllo-inositol (3.35 ppm).

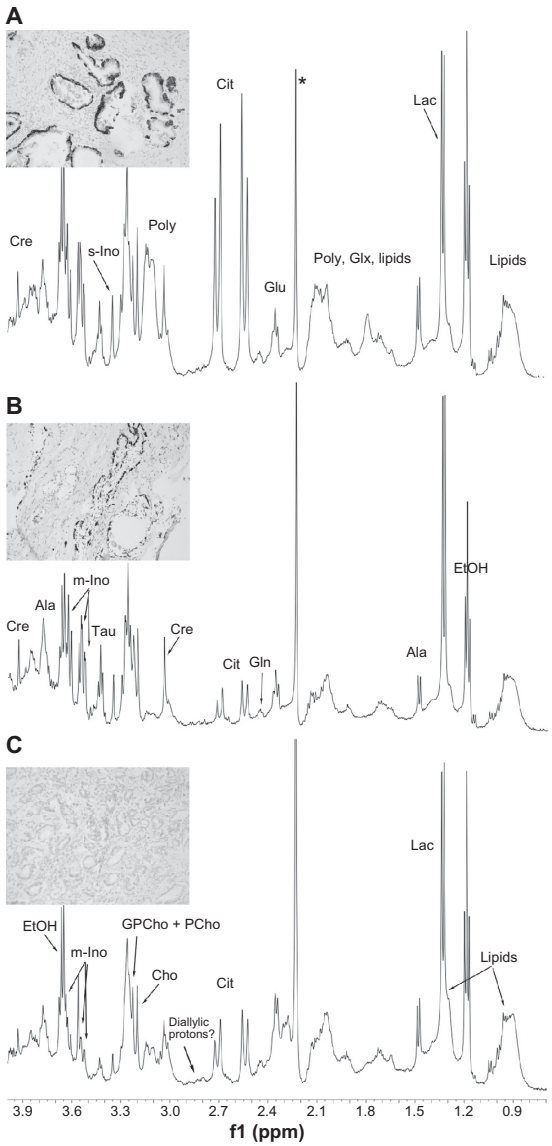

Figure 1. Representative ^{1}H MAS NMR spectra of **A**) Non-malignant; **B**) 10% malignant; **C**) 100% malignant human prostate tissue samples obtained from a 67-year-old patient with a serum PSA of 50 and a GS 7(3 + 4) stage 3 tumor. Inserted micrographs: To distinguish malignant and non-malignant glands the sections were immuno-stained to visualize basal epithelial cells (dark) lining non-malignant glands. **A**) 100% non-malignant prostate tissue sample with corresponding morphology. All glands are lined with a basal cell layer and are thus non-malignant; **B**) Malignant prostate sample containing 10% tumor and 90% non- malignant tissue. The malignant glands, seen in the middle left constitute 10% of the whole sample and lack basal cells; **C**) Prostate sample containing 100% cancer. In this specimen no basal cells can be seen.
Note: *Contaminant.

The NMR spectra contained quantitative information about the metabolites present in the examined prostate tissues. Basic descriptive data are presented in Table 1.

Further analysis of these data detected the correlations between the NMR-acquired information and the following cancer-related parameters:

Table 1. Mean metabolite ratios (±SD) of non-malignant and malignant prostate tissue samples.

Variable	Diagnosis	n	Mean	SD
Age	Non-malignant	108	60.36	5.59
	Malignant	41	59.37	5.41
Ki67	Non-malignant	108	0.04	0.30
	Malignant	37	3.91	3.70
PSA	Non-malignant	108	12.19	14.02
	Malignant	40	12.83	12.39
Distance to tumor	Non-malignant	108	1.00	1.01
	Malignant	41	0.00	0.00
Fraction of tumor in %	Non-malignant	108	0.00	0.00
	Malignant	41	41.85	33.60
Myo-Ino/Cre	Non-malignant	108	0.42	0.26
	Malignant	41	0.45	0.18
(GPCho + Pcho)/ Cre	Non-malignant	108	0.86	0.26
	Malignant	41	1.42	0.70
Cho/Cre	Non-malignant	108	1.15	0.52
	Malignant	41	1.93	1.87
Cit/Cre	Non-malignant	108	1.36	0.74
	Malignant	41	1.35	0.65
Myo-Ino/ scyllo-Ino	Non-malignant	108	5.65	1.59
	Malignant	41	4.98	1.75

Gleason scores

Binary multivariate logistic regression was used to assess the ability of NMR-measured metabolite ratios to differentiate between tumors with Gleason scores of 6 and 7. For malignant tissues, no single ratio had significant discriminatory power in this respect ($P = 0.081$ and OR 0.08 for the Cit/Cre ratio, the strongest predictor). In contrast, for non-malignant tissue samples (taken at various distances from the tumor) m-Ino/s-Ino and Cho/Cre ratios were both strongly related to the tumor Gleason score (OR 0.22, 95% CI 0.09–0.57, $P = 0.002$ and OR 12.8, 95% CI 3.57–45.75, $P < 0.001$, respectively). Mean values of metabolite ratios for both malignant and non-malignant prostate tissue specimens with Gleason Scores of 6 vs. GS 7 are presented in Table 2.

Tumor cell fractions in the samples

We have previously shown that HRMAS NMR-derived bio-markers can be used to discriminate between malignant and non-malignant prostate tissue.[21] As individual prostate needle biopsies often contain mixtures of both non-malignant and malignant tissue we have now examined the power of HRMAS NMR to determine the fraction of cancerous tissues in a mixed sample. The multivariate linear regression analysis demonstrated that the (GPCho + PCho)/Cre,

Table 2. Mean metabolite ratios (±SD) of prostate tissue samples according to Gleason score: malignant GS 6 (n = 27) vs. malignant GS 7 (n = 14), and non-malignant tissue adjacent to GS 6 (n = 85) vs. non-malignant tissue adjacent to GS 7 (n = 23).

Malignant	Gleason score	*n*	Mean	SD
(GPCho + PCho)/Cre	6	27	1.25	0.57
	7	14	1.74	0.81
Cho/Cre	6	27	1.71	1.87
	7	14	2.34	1.86
Cit/Cre	6	27	1.56	0.61
	7	14	0.93	0.51
m-Ino/s-Ino	6	27	5.34	1.75
	7	14	4.28	1.55
m-Ino/Cre	6	27	2.01	0.36
	7	14	2.03	0.49
Non-malignant				
(GPCho + PCho)/Cre	6	85	0.84	0.22
	7	23	0.92	0.33
Cho/Cre*	6	85	1.08	0.32
	7	23	1.41	0.89
Cit/Cre	6	85	1.33	0.70
	7	23	1.47	0.88
m-Ino/s-Ino*	6	85	6.07	1.41
	7	23	4.08	1.22
m-Ino/Cre	6	85	2.16	0.48
	7	23	1.99	0.36

Notes: Std. Err. Adj. for clustering, *$P \leq 0.05$.

m-Ino/s-Ino, Cho/Cre, and s-Ino/Cre mean ratios correlated with the tumor fraction (tumor load), in the specimens ($R^2 = 0.45$, $P < 0.05$; Table 3). The correlation of the most strongly related ratio, (GPCho + PCho)/Cre, with tumor load is displayed in Figure 2. It should be noted that specimens containing a particular fraction of tumor tissue showed substantially higher inter-sample variations in spectral values of (GPCho + PCho)/Cre, than non-malignant tissue samples (Fig. 2).

The morphology of non-malignant samples was however highly variable, eg, with respect to fractions of stroma and epithelium, the presence of inflammatory cells and glandular morphologies (atrophic or not). Such differences apparently had only moderate effects on the spectra derived from non-malignant tissue.

Number of proliferating cells

The metabolite ratio (GPCho + PCho)/Cre in tumor tissue correlated not only with tumor load, as described above, but also with the proliferation marker Ki67 (b = 1.97, SE b = 0.47, 95% CI 1.02–2.92, $R^2 = 0.15$, $P < 0.001$).

Distance to the nearest tumor

The distance to the nearest tumor was jointly correlated with the m-Ino/s-Ino and (GPCho + PCho)/Cre ratios ($R^2 = 0.09$), with the following parameters: m-Ino/s-Ino, b = 0.10, SE b = 0.04, 95% CI 0.01–0.18, $P = 0.03$; (GPCho + PCho)/Cre, b = –0.46, SE b = 0.11, 95% CI –0.68—0.22, $P < 0.001$. Although significant, this correlation is weak.

Discussion

We have demonstrated here that HRMAS NMR analyses of prostate tissues can provide valuable metabolomic information for determining the tumor load in prostate tissue samples. In addition, this information can be used to establish relationships between metabolite levels and disease aggressiveness, based on their relations to Gleason score, cell proliferation, and tumor stage. Furthermore, HRMAS NMR-derived information appears to be related to changes in non-malignant parts of prostates harbouring tumors that reflect the nature and proximity of the

Table 3. Summary of results obtained from the multivariate linear regression analysis. The likelihood of a tissue sample containing cancer tissue is significantly positively associated with an increased ratio of (GPCho + PCho)/Cre, and negatively associated with decreased ratios of m-Ino/s-Ino, Cho/Cre and s-Ino/Cre.

Multivariate linear regression dependent: fraction of tumor in per cent (0, 20, 40, 60, 80, 100%)					
Metabolite ratios	**B**	**Std. error**	***P***	**95% CI**	
(GPCho + PCho)/Cre	44.19	5.16	0.000	33.99	54.40
m-Ino/s-Ino	–4.37	1.23	0.001	–6.81	–1.90
Cho/Cre	–5.72	2.22	0.011	–10.12	–1.32
s-Ino/Cre	–23.24	8.69	0.008	–39.42	–6.16

Note: $R^2 = 0.45$. Std. Err. Adj. for clustering.

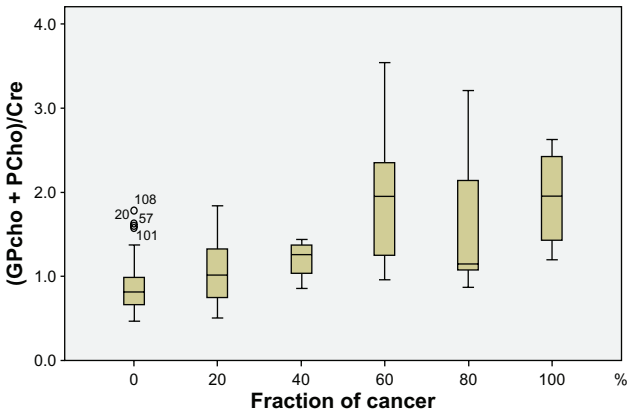

Figure 2. Box-Plot graph depicting the correlation between the (GPCho + PCho)/Cre metabolite ratio and the fraction of cancer tissue in the prostate samples.

tumors. Thus, such analysis could provide a powerful complementary means to examine diagnostic prostate needle biopsies, as suggested by van Asten and co-workers.[22]

In addition, malignant and non-malignant samples can be discriminated using the differences between them in spectral ratios of GPCho + PCho[23] and Cre,[21] as previously reported. Since they vary much less between stromal and glandular tissues, choline compounds (CC) are more useful for this purpose than citrate, which generally accumulates more in normal prostate epithelial cells than in both stroma and cancer cells.[24,25] Furthermore, statistical analyses involving citrate levels, particularly ratios between citrate and other metabolites, are complicated by its variability, especially if some samples have spectroscopically baseline levels so ratios have close to infinite values.[21,24,26] The variability and practical consequences of citrate were observed in our study, since the logistic regression analysis showed the Cit/Cre ratio to be significantly ($P = 0.010$) related to aggressiveness (tumor Gleason score) without adjusting for clustering, but non-significantly related ($P = 0.081$) after adjusting for clustering. Compared to citrate, the other biomarker and biomarker ratios tested in this study appeared to be more robust, which is clearly essential for biomarkers that are to be used clinically, since prostate biopsies have varying morphologies, stroma to epithelium ratios and pathologies, in addition to variations associated with cancer.[15]

Thus, the prostate gland is a challenging organ to study, and detailed knowledge of its structure and pathology as well as metabolism is essential when interpreting MR spectra.[21,27] Furthermore, an important feature of PCa is that malignant cells often infiltrate among non-malignant glands so "tumor samples", such as those examined in this study, that may be assumed to be pure tumor according to their position in a whole-mount section, often prove to be mixtures of malignant and non-malignant tissues on closer examination. Small increases in the (GPCh + PCho)/Cre ratio proved, in this study, to be valuable indicators of the presence and fraction of cancer cells, as can be seen in Tables 1 and 3. A previous breast cancer study showed that GPCho and PCho resonances can be separated using high-field (600 Mhz) HRMAS NMR, and that increases in PCho relative to Cho are indicative of cancer.[28] Our study did not allow such detailed exploration of the prostate tissue samples, due to the broad range in tumor load in the 41 malignant specimens (Fig. 2). Therefore, an increase in the spectral resolution might have added further diagnostic strength to the correlations between bio-markers and tumor load in our study. The (GPCh + PCho)/Cre ratio proved to have additional strengths as an indicator for PCa as it correlated weakly, but significantly, to the Ki67 index (and thus tumor cell proliferation) in our study. However, to verify our findings and validate their use in clinical diagnostics, studies including a larger number of patients and specimens with a wider range of tumor morphologies are required.

Increases in choline compounds, probably due to increased turnover of cell membranes, are well known markers of cancer,[15,28,29] particularly cancers with high Gleason scores.[30] The Gleason score is the best prognostic indicator currently available,[31] thus it is of great interest to assess robust biomarkers which relate to PCa aggressiveness graded by the GS. Spectroscopic biomarkers with correlative properties to aggressiveness include choline compounds (CC), Cit/Cre, Cho/Cre, (tCho + Cre)/Cit and tCho/Cre.[15,22,29,32] However, according to our multivariate analysis, after adjusting for clustering the biomarker that proved to be the strongest potential candidate for differentiating between GS 6 and 7 tissues was the Cit/Cre ratio, not a CC. This observation corroborated findings from a previous examination of prostate needle biopsies.[22]

We have recently published indications that prostate tumors in both experimental models and patients

influence the surrounding non-malignant prostate tissue, and that the strength of this influence is related to tumor size and aggressiveness.[17] Thus, the prostate appears to be "tinted" by the presence and nature of cancer elsewhere in the organ, and we proposed that this indication of cancer in non-malignant tissue can be named "TINT". Other investigators have suggested that observed alterations in non-malignant tissue surrounding prostate tumors are the result of a "cancer field" effect.[33] In the present study we found that HRMAS NMR can detect changes in m-Ino/s-Ino, and Cho/Cre ratios in non-malignant tissue that are related to disease aggressiveness, i.e., changes that can differentiate between samples from prostates with relatively indolent Gleason score 6 or more aggressive Gleason score 7 tumors.[34] Moreover, the spectral ratios of (GPCho + PCho)/Cre and m-Ino/s-Ino in non-malignant samples were weakly, but significantly, jointly related to the distance to the nearest tumor in the prostate gland. This is potentially important since needle biopsies are taken from the organ when prostate cancer is suspected, as a result of symptoms and or increased serum PSA, but prostate tumors are difficult to visualize using current imaging techniques so biopsies may miss the tumor. Indeed prostate biopsies from at least 75% of all men with prostate tumors show no signs of cancer.[17] If, however, it was possible to detect changes in such apparently normal biopsies, using HRMAS NMR or other methods, we may be able to predict the risk that an aggressive tumor is present elsewhere in the organ and, hence, the need for additional biopsies. Interestingly, a previous study has also suggested that clinical MRS examination of non-malignant parts of the prostate can be used to determine prostate cancer aggressiveness.[29]

Another potentially interesting NMR-detectable biomarker identified in our multivariate analysis was the dietary phytochemical, anti-oxidant, osmolyte, and carbohydrate inositol.[35] Inositol, or myo-inositol, and its various biochemical derivatives, are readily found in mammalian cells and organs, including the brain, kidney, secretory tissues, testis, epididymal, vesicular, and prostatic fluid, and is involved in various aspects of reproduction.[35–38] Myo-inositol is synthesized from glucose 6-phosphate by myo-inositol-3-phosphate synthase (IP synthase) in most tissues, however, there are several IP synthase isoforms, in both rats and humans, suggesting that inositol biosynthesis by IP synthase is a highly regulated and multifaceted process.[38]

Myo-inositol is the parent compound of phytic acid, or inositol hexaphosphate (IP6). Jointly, these compounds, which are readily found in legumes, and fibre-rich foods, have received much attention lately due to their potential anti-carcinogenic and protective properties, both general[39,40] and specifically for PCa.[41–44] Scyllo-inositol, also detected in our study, is a myo-Inositol isomer that (interestingly) is under investigation for its potential use following derivatization as a novel Positron Emission Tomography (PET) radiotracer, [18F]-1-deoxy-1-fluoro-scyllo-inositol, for both breast cancer and Alzheimer's disease (AD).[44,45] Both scyllo-inositol and myo-inositol are components of the prostate metabolite profile generated by HRMAS NMR[15] and profiles of both lung tumors[46] and colon cancer.[47] However, the m-Ino/s-Ino ratio has not been previously studied, to our knowledge, although our findings indicate that it is negatively correlated with aggressiveness (in non-malignant prostate tissue samples) and tumor load and, conversely, positively correlated to non-malignancy. Hence, malignancy appears to be associated with reductions in the concentration of myo-Inositol and/or increases in the concentration of scyllo-Inositol (Fig. 1A–1C).

Conclusions

The ^{1}H HRMAS NMR approach appears to have the potential to determine if a cancer may be present in the proximity of non-malignant prostate tissue biopsies. In addition, analysis of prostate tissue samples can be used to determine the fraction of tumor cells in a prostate tissue biopsy. Further explorations of additional HRMAS NMR detectable metabolites are needed to increase the capacity to distinguish different types of samples and to elucidate the potential of using spectroscopic biomarkers that can be examined clinically in the future.

Acknowledgements

Support by the Lion's Cancer Research Foundation (grant no. AMP08-565), Umeå University, the Swedish Cancer Foundation and Swedish Research Council is gratefully acknowledged. Thanks are due to Birgitta Ekblom, Elisabeth Dahlberg, Pernilla

Andersson (Dept. of Medical Biosciences, Pathology), Kerstin Almroth and Britt-Inger Dahlin (Dept. of Surgical and Perioperative Sciences).

Abbreviations

HRMAS, high-resolution magic angle spinning; NMR, nuclear magnetic resonance; PCa, prostate cancer; (GPCho + PCho), glycerophosphorylch oline + phosphorylcholine; Cho, choline; m-Ino, myo-inositol; s-Ino, scyllo-inositol; Cre, creatine; Cit, citrate.

Disclosure

This manuscript has been read and approved by all authors. This paper is unique and is not under consideration by any other publication and has not been published elsewhere. The authors and peer reviewers of this paper report no conflicts of interest. The authors confirm that they have permission to reproduce any copyrighted material.

References

1. Thun MJ, DeLancey JO, Center MM, Jemal A, Ward EM. The global burden of cancer: priorities for prevention. *Carcinogenesis*. 2010;31(1):100–10.
2. Wolf AMD, Wender RC, Etzioni RB, Thompson IM, D'Amico AV, et al. American Cancer Society Guideline for the Early Detection of Prostate Cancer. *CA Cancer J Clin*. 2010;60:70–98.
3. Chrouser KL, Lieber MM. Extended and saturation needle biopsy for the diagnosis of prostate cancer. *Curr Urol Rep*. 2004;5(3):226–30.
4. Fleshner N, Klotz L. Role of "saturation biopsy" in the detection of prostate cancer among difficult diagnostic cases. *Urology*. 2002;60:93–7.
5. Baccala AA, Moussa AS, Elbary AA, et al. Risk factors and predictors of prostate cancer in men with negative repeat saturation biopsy. *Uro Today Int J*. 2010;3(1).
6. Tessem MB, Selnaes KM, Sjursen W, et al. Discrimination of patients with microsatellite instability colon cancer using 1H HR MAS MR spectroscopy and chemometric analysis. *J Proteome Res*. 2010;9(7): 3664–70.
7. Santos CF, Kurhanewicz J, Tabatabai ZL, et al. Metabolic, pathologic, and genetic analysis of prostate tissues: quantitative evaluation of histopathologic and mRNA integrity after HR-MAS spectroscopy. *NMR Biomed*. In press.
8. Levin YS, Mark J. Albers MJ, et al. Methods for metabolic evaluation of prostate cancer cells using proton and ^{13}C HR-MAS spectroscopy and [3–^{13}C] pyruvate as a metabolic substrate. *Magn Reson Med*. 2009;62: 1091–8.
9. Shukla-Dave A, Hricak H, Ishill N, et al. Prediction of prostate cancer recurrence using magnetic resonance imaging and molecular profiles. *Clin Cancer Res*. 2009;15(11):3842–9.
10. Lange T, Schulte RF, Boesiger P. Quantitative J-resolved prostate spectroscopy using two-dimensional prior-knowledge fitting. *Magn Reson Med*. 2008;59(5):966–72.
11. Cheng LL, Lean CL, Bogdanova A, et al. Enhanced resolution of proton NMR spectra of malignant lymph nodes using magic-angle spinning. *Magn Reson Med*. 1996;36:653–8.
12. Sitter B, Sonnewald U, Spraul M, Fjösne H, Gribbestad IS. High-resolution magic angle spinning MRS of breast cancer tissue. *NMR Biomed*. 2002; 15(5):327–37.
13. Beckonert B, Coen M, Keun HC, et al. High-resolution magic-angle-spinning NMR spectroscopy for metabolic profiling of intact tissues. *Nature Protocols*. 2010;5:1019–32.
14. Gleason DF, Mellinger GT. Prediction of prognosis for prostatic adenocarcinoma by combined histological grading and clinical staging. *J Urol*. 1974;111:58–64.
15. Swanson MG, Vigneron DB, Tabatabai ZL, et al. Proton HR-MAS spectroscopy and quantitative pathologic analysis of MRI/3D-MRSI targeted post-surgical prostate tissues. *Magn Reson Med*. 2003;50(5):944–54.
16. Josefsson A, Wikström P, Granfors T, et al. Tumor size, vascular density and proliferation as prognostic markers in GS 6 and GS 7 prostate tumors in patients with long follow-up and non-curative treatment. *Eur Urol*. 2005; 48(4):577–83.
17. Halin S, Hammarsten P, Adamo H, Wikstrom P, Bergh A. Tumor indicating normal tissue (TINT) could be a novel source of diagnostic and prognostic markers for prostate cancer. *Expert Opinion on Medical Diagnostics*, 2011,5(01):37–47.
18. Meiboom S, Gill D. Modified spin-echo method for measuring nuclear relaxation times, Rev. *Sci Instrum*. 1958;29:688–91.
19. Jordan KW, He W, Halpern EF, Wu C-L, Cheng LL. Evaluation of tissue metabolites with high resolution magic angle spinning MR spectroscopy human prostate samples after three-year storage at –80 °C. *Biomarker Insights*. 2007;2:147–54.
20. Stenman K, Hauksson JB, Gröbner G, Stattin P, Bergh A, Riklund K. Detection of polyunsaturated omega-6 fatty acid in human malignant prostate tissue by 1D and 2D high-resolution magic angle spinning NMR spectroscopy. *MAGMA*. 2009;22(6):327–31.
21. Stenman K, Surowiec I, Antti H, et al. Detection of local prostate metabolites by HRMAS NMR spectroscopy: A comparative study of human and rat prostate tissues. *Magnetic Resonance Insights*. 2010;4:27–41.
22. Van Asten J, Cuijpers V, Hulsbergen-van de Kaa C, et al. High resolution magic angle spinning NMR spectroscopy for metabolic assessment of cancer presence and Gleason score in human prostate needle biopsies. *Magn Reson Mater Phy*. 2008;21:435–42.
23. Swanson MG, Zektzer AS, Tabatabai ZL, et al. Quantitative analysis of prostate metabolites using ^{1}H HR-MAS spectroscopy. *Magn Reson Med*. 2006;55(6):1257–64.
24. Swindle P, McCredie S, Russell P, et al. Pathologic characterization of human prostate tissue with proton MR spectroscopy. *Radiology*. 2003;228: 144–51.
25. Singh KK, Desouki MM, Franklin RB, Costello LC. Mitochondrial aconitase and citrate metabolism in malignant and nonmalignant human prostate tissues. *Mol Cancer*. 2006;5:14.
26. McLean MA, Barrett T, Gnanapragasam VJ, et al. Prostate cancer metabolite quantification relative to water in ^{1}H-MRSI in vivo at 3 Tesla. *Magn Reson Med*. In print. 2010.
27. Swindle P, Ramadan S, Stanwell P, McCredie S, Russell P, Mountford C. Proton magnetic resonance spectroscopy of the central, transition and peripheral zones of the prostate: assignments and correlation with histopathology. *Magn Reson Mater Phy*. 2008;21:423–34.
28. Sitter B, Lundgren S, Bathen TF, Halgunset J, Fjosne HE, Gribbestad IS. Comparison of HR MAS MR spectroscopic profiles of breast cancer tissue with clinical parameters. *NMR Biomed*. 2006;19:30–40.
29. Cheng LL, Burns MA, Taylor JL, et al. Metabolic characterization of human prostate cancer with tissue magnetic resonance. *Cancer Res*. 2005;65: 3030–4.
30. Kurhanewicz J, Swanson MG, Nelson SJ, Vigneron DB. Combined magnetic resonance imaging and spectroscopic imaging approach to molecular imaging of prostate cancer. *J Magn Reson Imaging*. 2002;16:451–63.
31. Kelloff GJ, Choyke P, Coffey DS. Challenges in clinical prostate cancer: *Role of Imaging AJR*. 2009;192:1455–70.
32. Zakian KL, Sircar K, Hricak H, Chen H-N, Shukla-Dave A, Eberhardt S. Correlation of proton MR Spectroscopic Imaging with Gleason Score Based on Step-Section Pathologic Analysis after Radical Prostatectomy. *Radiology*. 2005;234:804–14.
33. Nonn L, Ananthanarayanan V, Gann PH. Evidence for field cancerization of the prostate. *Prostate*. 2009;69(13):1470–9.

34. Egevad L, Granfors T, Karlberg L, Bergh A, Stattin P. Prognostic value of the Gleason score in prostate cancer. *BJU Int*. 2002;89(6):538–42.
35. Patricia Beemster P, Groenen P, Steegers-Theunissen R. Involvement of inositol in reproduction. *Nutrition Reviews*. 2002;60(3):80–7.
36. Lewin LM, Yannai Y, Sulimovici S, Kraicer PF. Studies on the metabolic role of myo-inositol. Distribution of radioactive myo-inositol in the male rat. *Biochem J*. 1976;156:375–80.
37. Mann T. Secretory function of the prostate, seminal vesicle and other male accessory organs of reproduction. *J Reprod Fert*. 1974;37:179–88.
38. Seelan RS, Lakshmanan J, Casanova MF, Parthasarathy RN. Identification of myo-inositol-3-phosphate synthase isoforms. Characterization, expression, and putative role of a 16-kDa γc isoform. *JBC*. 2009;284:9443–57.
39. Vucenik I, Shamsuddin AM. Cancer inhibition by inositol hexaphosphate (IP6) and inositol: from laboratory to clinic. *J Nutr*. 2003;133(11 Suppl 1): 3778S–84.
40. Bacić I, Druzijanić N, Karlo R, Skific I, Jagić S. Efficacy of IP6 + inositol in the treatment of breast cancer patients receiving chemotherapy: prospective, randomized, pilot clinical study. *J Exp Clin Cancer Res*. 2010;29:12.
41. Singh RP, Agarwal C, Agarwal R. Inositol hexaphosphate inhibits growth, and induces G1 arrest and apoptotic death of prostate carcinoma DU145 cells: modulation of CDKI-CDK-cyclin and pRb-related protein-E2F complexes. *Carcinogenesis*. 2003;24(3):555–63.
42. Singh RP, Sharma G, Mallikarjuna GU, Dhanalakshmi S, Agarwal C, Agarwal R. In vivo suppression of hormone-refractory prostate cancer growth by inositol hexaphosphate. Induction of insulin-like growth factor binding protein-3 and inhibition of vascular endothelial growth factor. *Clin Cancer Res*. 2004;10:244.
43. Roy S, Gu M, Ramasamy K, et al. p21/Cip1 and p27/Kip1 are essential molecular targets of inositol hexaphosphate for its antitumor efficacy against prostate cancer. *Cancer Res*. 2009;69(3):1166–73.
44. Gu M, Roy S, Raina K, Agarwal C, Agarwal R. Inositol hexaphosphate suppresses growth and induces apoptosis in prostate carcinoma cells in culture and nude mouse xenograft: PI3K-Akt pathway as potential target. *Cancer Res*. 2009;69(24):9465–72.
45. Vasdev N, Chio J, van Oosten EM, et al. Synthesis and preliminary biological evaluations of [18F]-1-deoxy-1-fluoro-scyllo-inositol. *Chem Commun (Camb)*. 2009;(37):5527–9.
46. Pimlott SL, Sutherland A. Molecular tracers for the PET and SPECT imaging of disease. *Chem Soc Rev*. 2011;40(1):149–62.
47. Duarte IF, Rocha CM, Barros AS, Gil AM, Goodfellow BJ, Carreira IM, et al. Can nuclear magnetic resonance (NMR) spectroscopy reveal different metabolic signatures for lung tumors? *Virchows Arch*. 2010;457:715–25.